Design Guidelines for FRP-Faced Foam Core Sandwich Panels: Review and Building Code Compliance

Raghad Kassab[1] and Pedram Sadeghian[2]

[1]PhD Candidate in Civil Engineering, Department of Civil and Resource Engineering, Dalhousie University, 1360 Barrington St., Halifax, NS, B3H 4R2 Canada. E-mail: R.kassab@dal.ca (corresponding author)

[2]Associate Professor and Canada Research Chair in Sustainable Infrastructure, Department of Civil and Resource Engineering, Dalhousie University, 1360 Barrington St., Halifax, NS, B3H 4R2 Canada. E-mail: pedram.sadeghian@dal.ca

ABSTRACT:

This paper presents a detailed review of structural insulated panels (SIPs), specifically focusing on variants composed of fiber-reinforced polymer (FRP) facings and foam core, and their applications within the construction industry, with a particular emphasis on compliance with Canadian building codes. The discussion encompasses the historical evolution of SIPs, fundamental design criteria, and their structural and thermal performance. Traditional SIPs, typically comprising an insulating foam core sandwiched between oriented strand board (OSB) facings, are reviewed alongside non-traditional FRP-faced SIPs. The latter's preliminary design considerations, emphasizing optimized foam core thickness and density to enhance thermal insulation without compromising structural integrity under diverse load conditions, are explored. Challenges and solutions associated with integrating SIPs into construction practices are addressed, highlighting the absence of universally recognized building codes specifically tailored for SIP design. Efforts to bridge this gap through detailed compliance pathways with the North American building codes are discussed. Furthermore, the paper delves into panel connections and overall system performance, focusing on achieving both thermal efficiency and structural integrity. Design examples showcasing the

utilization of FRP-faced SIPs in various structural components, including floors, roofs, and walls, are provided. These examples detail load-bearing capacity, deflection limits, and the implementation of design principles to ensure optimal performance.

DOI: https://doi.org/10.1061/JAEIED.AEENG-1920

KEYWORDS: Sandwich Panels; FRP-Faced SIPs; Design Compliance; Structural Engineering; Innovative Building Materials.

1. INTRODUCTION

Introduced in the 1930s, structural insulated panels (SIPs)—also referred to as stressed skin panels or structural sandwich panels—have progressively gained attention in the building industry (Amran et al, 2020). Their widespread use has been limited and restrained, however, due to the lack of universally recognized building codes tailored to SIP design and application, causing hesitancy among builders (Moynihan, 2014). These panels consist of two stiff facings: oriented strand board (OSB), used to resist bending force; and a low-density core such as expanded polystyrene (EPS) or polyurethane (PUR) to resist shear forces and provide insulation (Yang and Rungthonkit, 2009). In residential construction, SIPs are recognized for their effectiveness in constructing floors, walls, and roofs across diverse projects (Koones, 2013). Beyond the traditional materials, there exist non-traditional SIPs that incorporate innovative facing materials like fiber-reinforced polymer (FRP) composites (Reis and Rizkalla, 2008; Fam and Sharaf, 2010; Manalo et al., 2016; Thakur et al., 2017)—offering greater stiffness compared to OSB or wood and, therefore less thickness is required for the facing to resist bending—and innovative core materials such as polyethylene terephthalate (PET) (Garrido and Correia, 2018; Xie et al., 2022; Kassab and Sadeghian, 2023) or polyvinyl chloride (PVC) foam (Mostafa et al., 2014; Zhou, 22019). Further research into bio-based sandwich beams with paper honeycomb cores and studies on corrugated cardboard as viable core materials underscore the potential of these environmentally friendly options to enhance the sustainability of building materials (McCracken & Sadeghian, 2018; Fu & Sadeghian, 2020, 2023). Figure 1 illustrates a comparison of these discussed SIP types: part (a) demonstrates a traditional SIP, and part (b) illustrates a non-traditional SIP. Recently, the use of flax FRP (FFRP) as an eco-friendly alternative to traditional glass FRP (GFRP) facings in SIPs demonstrated comparable strength and introduced sustainable material options into the building industry (Hristozov et al., 2016; CoDyre and Fam, 2017; Betts et al., 2018).

Regardless of the materials type used for facings and core, the upfront cost of SIPs appears substantial, which can be mitigated, however, by potential long-term savings, particularly regarding energy or electricity costs (McCullom and Krarti, 2010). The advantage becomes pronounced in areas experiencing significant temperature variances between interior and exterior environments. Despite both SIPs and traditional stud-based constructions needing to meet resistance value R-value —thermal resistance standards set by organizations under guidelines from energy and building codes—SIPs often outperform in thermal efficiency. Their continuous foam core eliminates thermal bridging—a common issue in stud constructions where studs create intermittent gaps in insulation (Kelley and Blanford, 2023). However, it is critical to note that the enhanced thermal insulation provided by SIPs' continuous foam core also depends significantly on maintaining airtight connections between the panels and at critical junctions such as floor-wall and roof-wall interfaces. Ensuring airtightness is vital for maximizing the system's overall energy efficiency.

With an advantage highlighted by Robert Snow Means (RSMeans) research (Drain et al., 2006), SIPs significantly enhance construction efficiency and can decrease labour hours by approximately 55% compared to traditional stud systems. As a result, efficiency accelerates construction and offsets the higher initial costs associated with SIP installation, which may involve specialized equipment (like cranes). A balance between initial investment and long-term savings helps position SIPs as a preferred choice in contemporary building projects, blending practical advantages with proven cost-effectiveness. According to a recent report, the global market for SIPs is expected to grow in value from US$ 443.2 million in 2023 to US$ 728.8 million by 2033 at a compound annual growth rate (CAGR) of 5.1% (Fact.MR., 2023). This growth is driven by increasing international investments in energy-efficient infrastructure and a rising demand for cold storage solutions. Consequently, despite proven efficiency and cost-effectiveness, the broader adoption of SIPs is still challenged by the absence of specific building codes dedicated to their simplified design process coupled with builders' limited use and experience. This highlights the need for design guidelines to fully comprehend SIP's potential in facilitating energy-efficient construction.

2. COMPLIANCE WITH BUILDING CODES

The integration of SIPs into construction projects requires a careful approach to align with building codes such as the International Building Code (IBC) in the United States and the National Building Code of Canada (NBCC), both of which provide limited specific guidance for SIPs compared to traditional wood-frame construction covered under the International Residential Code (IRC) and Part 9 of the NBCC, which addresses "Housing and Small Buildings." Compliance can be achieved through prescriptive methods detailed in these codes or through performance-based approaches.

In the U.S., international code council (ICC) AC04 outlines the acceptance criteria for sandwich panels, ensuring SIPs meet the necessary safety and performance standards. In Canada, the NBCC provides two primary avenues for achieving compliance. The first is prescriptive compliance, which mandates adherence to the acceptable solutions outlined in Division B, ensuring each SIP system component aligns with established benchmarks. Secondly, a performance-based path that offers the flexibility to propose innovative applications not explicitly covered in the code. These solutions must still meet the requisite performance levels as determined by the objectives and functional statements in Division B. Therefore, the SIP design process involves and requires a thorough analysis of structural loads and thermal insulation standards—as mandated by the NBCC and the National Energy Code of Canada for Buildings (NECB)—to promote energy efficiency across diverse Canadian climates.

For projects using new forms of SIPs, the Canadian Construction Materials Centre (CCMC) in Canada and the National Testing Agency (NTA) in the U.S. provide evaluations to certify the acceptability for construction use, pending approval by the local Authority Having Jurisdiction (AHJ). However, financial and logistical challenges may deter new companies from pursuing CCMC or NTA certification. It is feasible to employ SIPs based on direct compliance with the code criteria, provided the necessary engineering analyses and documentation substantiate the product's standards. Ultimately, local building officials assess compliance, and while certifications from CCMC and NTA enhance marketability, their absence does not deny the possibility of approval through alternative demonstrations.

3. DESIGN EQUATIONS OF FRP-FACED SIPS

3.1 Thermal Insulation: Core Thickness

A foundational step in designing FRP-faced SIPs focuses on establishing core thickness, a factor that influences the panel's thermal insulation performance. This process begins by understanding that thermal insulation—quantified by the R-value—is directly linked to core thickness and thermal conductivity, which is a primary determinant of a material's insulative capacity. This R-value can be calculated by dividing the material thickness by its thermal conductivity, highlighting the role of thermal conductivity as a primary determinant of a material's insulative capacity. While density is often predetermined and influences the thermal conductivity, the optimization of the core's cross-section primarily aims to enhance, which can range from 1 to 2 per inch thickness and vary according to the foam material used.

In adhering to North American insulation standards, including both Canadian and U.S. codes, designers must conduct a thorough analysis of climate-specific requirements. For the Canadian context, illustrated in Figure A-1.1.4.1.(1) of the NECB, a contour map analysis of the energy code shows an average annual heating degree-days of 18˚C for various Canadian cities, and analysis leads to the identification of the project's climate zone. Subsequently, the process involves reviewing the energy code's guidelines for the maximum allowable thermal transmittance for building envelopes—including walls, roofs, and floors—tailored to each climate zone. These specifications are essential for evaluating insulation effectiveness.

Transitioning to the United States, compliance with the International Energy Conservation Code (IECC) involves a similar analysis to categorize regions based on their climate conditions. Here, the IECC specifies maximum allowable U-factors for different building components, tailored per climate zone, essential for assessing the effectiveness of insulation materials. The U-factor, measures the rate of heat transfer through a building component, indicating the effectiveness of the material's insulation properties.

The ability of FRP-faced SIPs to meet the mentioned standards hinges on the thermal conductivity of the core, which differs according to the core material's density. A direct relationship exists where higher density leads to increased thermal conductivity, thereby reducing the panel's insulating capability. This highlights the critical role of selecting the right core density to achieve optimal insulation levels while ensuring structural integrity. Once density is determined, calculating the minimum FRP-faced SIP thickness needed to meet thermal insulation standards involves dividing the core's thermal conductivity by the climate zone's maximum thermal transmittance value. The calculated thickness aims to fulfill the thermal insulation criteria and often preempts compliance with structural strength and deflection standards for the panel.

3.2 Structural Strength under Transverse Loading: Facing thickness

Another critical aspect of FRP-faced SIP design is the calculation of facing thickness and its impact on structural strength. Contrary to common belief, increased facing thickness does not inherently enhance the SIP's bending strength due to potential issues, including core shear or wrinkling. Instead, it necessitates a comprehensive design approach that considers various potential failure modes to ensure an efficient and robust design.

This phase involves reviewing project details, including location, construction type (e.g. residential or commercial), and SIP specifications ranging from traditional OSB-faced panels with foam cores to innovative GFRP-faced panels with various core types. This information allows the determination of design distributed load values—such as live, wind, and snow loads—from Part 4 of the NBCC or chapter 16 of the IBC. Upon identifying the load-bearing standards from either NBCC or IBC, relying solely on the analysis of mechanics of materials for designing SIPs might not satisfy the design criteria set by building officials, who often mandate comprehensive testing to verify that SIPs can endure anticipated loads. This requirement is rooted in mitigating risks including premature failure or debonding, which mechanics of materials equations might not fully address. Consequently, while initial SIP designs are formulated using mechanics of materials principles—including sandwich theory to specify core and facing thicknesses—comprehensive designs for real-world applications require extensive testing.

The analysis involves calculating the maximum bending moment (*M*) and shear force (*V*) that FRP-faced SIPs should resist under a uniformly distributed factored load (*w*). By applying this load across the span length (*L*), and assuming simply supported boundary conditions, the panels' ultimate shear is $\pm\frac{\mathrm{w}\cdot\mathrm{L}}{2}$. Concurrently, the maximum bending moment—specifically at the midspan—is equivalent to $\mathrm{M} = \frac{\mathrm{w}\cdot\mathrm{L}^2}{8}$. These essential calculations are pivotal for evaluating the three critical failure modes pertinent to sandwich structures: face rupture, core shear, and wrinkling (the local buckling of the compression face).

3.2.1 Face rupture failure

Considering the face rupture mode, the internal bending moment is represented by $M = F \cdot d$, where "*F*" denotes the tension or compression force resisted by the facing during bending, and "*d*" denotes the distance between the mid-thickness of the sandwich facings, calculated as the sum of the facing thickness (t_f) and the core thickness (t_c). This calculation exclusively focuses on the face sheets, which are primarily responsible for bearing bending stresses due to their higher stiffness and strength relative to the core. In line with Allen's established assumptions, for simplification, when the core material's stiffness is significantly lower than that of the face sheets, the core's flexural contribution is considered negligible (Allen, 1969). This is quantitatively expressed by the criterion $4 \cdot \frac{E_f}{E_c} \cdot \frac{t_f}{t_c} \cdot \frac{d}{t_c} > 100$, where E_f and E_c are the moduli of elasticity for the facings and core, respectively.

Figure 2 illustrates the cross-section of a sandwich panel, highlighting its structural components used in these calculations. Substituting "*F*" with the product of the rupture stress in the facing (σ_{fu}) and the area of the facing leads to a simplified equation: $M = \sigma_{fu} \cdot t_f \cdot b \cdot d$. Incorporating the ultimate moment calculated for a uniformly distributed load, the equation is derived to determine the maximum distributed load a structure can withstand prior to initiating face rupture (w_{FR}):

$$w_{FR} = \frac{8\sigma_{fu} \cdot t_f \cdot b \cdot d}{L^2} \quad (1)$$

3.2.2 Face wrinkling failure

For the wrinkling mode of failure, the analysis turns to literature (Zenkert, 1997), identifying the stress causing wrinkling, σ_{WR}, as a function of the facing's modulus of elasticity , the core's modulus , and the core's shear modulus (G_c), summarized by $\sigma_{WR} = 0.5\sqrt[3]{E_f \cdot E_c \cdot G_c}$. Material compatibility is crucial to prevent this failure mode. If the facing modulus is significantly higher than the core modulus—suggesting a stiff-facing material not complemented by a similarly stiff core—the load causing face rupture may be high but is theoretical as local buckling or wrinkling becomes the dominant failure mode at a lower transversely applied load. The ultimate distributed load that could induce wrinkling (w_{WR}) is then calculated, like the approach for face rupture, but incorporates the wrinkling stress to derive: $w_{WR} = \frac{8\sigma_W \cdot t_f \cdot b \cdot d}{L^2}$, which further simplifies to:

$$w_{WR} = \frac{4\sqrt[3]{E_f \cdot E_c \cdot G_c} \cdot t_f \cdot b \cdot d}{L^2} \quad (2)$$

3.2.3 Core shear failure

The core shear failure mode analysis circles back to the previously determined maximum factored shear force due to bending, with a focus on the shear stress borne by the core. This section of the analysis is particularly concerned with the core's vulnerability to shear failure due to its significantly lower modulus of elasticity and shear strength compared to the facings.The shear force (V) is the product of the core's shear stress (τ_c) stress and its effective cross-sectional area, leading to the equation: $V = (t_c + t_f) \cdot b \cdot \tau_c$. From this basis, the equation for the critical uniform load that can induce core shear failure (w_{CS}) is defined as:

$$w_{CS} = \frac{2\tau_c \cdot b \cdot d}{L} \tag{3}$$

Given the negligible contribution of the core's stiffness to the overall flexural rigidity of the sandwich panels, the analysis is simplified to assume that the shear stress across the core's thickness remains constant (Allen, 1969). Ultimately, in assessing potential failure modes—face rupture, core shear, and wrinkling—the definitive failure mode yields the lowest uniform load for a specific span and cross-sectional dimensions of the SIP, while the remaining modes become hypothetical. These calculations are instrumental in identifying the most efficient facing thickness, balancing strength with material economy.

3.2.4 Deflection

Upon determining the cross-sectional properties of the FRP-faced SIP based on bending strength and thermal insulation considerations, the design process advances to assess the displacement response under load. This evaluation is crucial to ensure that the design meets the IBC and NBCC's deflection criteria outlined by serviceability limit state (SLS) standards. These codes dictate that deflection should not exceed the span length divided by specific ratios—120, 180, 240, or 360—based on the structural component and its application. Increasing the thickness of the facing material emerges as a primary strategy to mitigate deflection should the initial cross-sectional configuration not satisfy these deflection limits.

The deflection of a sandwich beam or a SIP under a uniformly distributed load, w, and simply supported conditions—as illustrated in Figure 3 (a)—comprises both bending deflection, Δ_B, and shear deflection, Δ_S, as depicted in Figures 3 (b) and (c), respectively. Bending deflection is calculated with $\Delta_B = \frac{5w \cdot L^4}{384D} = \frac{5w \cdot L^4}{192b \cdot d^2 \cdot t_f \cdot E_f}$, while shear deflection is determined by the equation

$\Delta_S = \frac{M_{max}}{A \cdot G} = \frac{w \cdot L^2 \cdot t_c}{8b \cdot d^2 \cdot G}$. These equations are simplified classic formulations attributed to Allen (1969), where "*A*" is expressed as $\frac{b \cdot d^2}{t_c}$ for shear deflection simplification, "*G*" denotes the shear modulus of the core, and *A·G* is recognized as "shear stiffness." Allen also notes that if the sandwich structure (referred to as a panel) is wide (i.e., the width "*b*" is much larger than the core thickness t_c) then when calculating the bending deflection, E_f should be replaced with $\frac{E_f}{(1-\nu_f^2)}$ if the wide sandwich panel is assumed to bend cylindrically. In which ν_f, represents the Poisson's ratio of the facing material. If it is assumed to bend anticlastic, then E_f remains unchanged. Additionally, for narrow sandwich structure (i.e., the width b is less than the core thickness t_c) then E_f is also not modified.

Based on both theoretical and empirical analysis, this design approach is essential for the initial development of panel designs. Subsequently, the designed FRP-faced SIP undergoes full-scale testing to validate efficacy and performance in real-world scenarios before implementation or approval by the jurisdiction. This imperative testing ensures effectiveness and suitability for real-world conditions before clearance for use. It aims to identify and rectify potential issues. This includes debonding, which is not predicted by analytical models and could lead to premature failure.

3.3 Structural Strength Under Axial Loading

In the context of axial loading, the structural performance of FRP-faced SIPs is closely linked to material composition and design details. The stiffness of the facing and core materials primarily affects the susceptibility of crushing failure and local buckling failure, whereas the global buckling failure mode is influenced by the panel's length and cross-sectional thickness. Recent studies demonstrated that increasing the core's density from 32kg/m³ to 64kg/m³, and then to 96kg/m³, markedly enhances the axial strength of SIPs with FFRP facings and polyisocyanurate (PIR) foam cores (CoDyre and Fam, 2017). This adjustment in core density can lead to significant increases in peak axial loads, with improvements of up to 76% for a single layer of FFRP and up to 176% for five layers. Additionally, axial strength reduces as the panel length increases from 500 mm to 1500 mm, whereas panels longer than 1250 mm are especially prone to global buckling. This insight points to enhancing core density as an effective method for improving axial strength, distinguishing it from strategies focused on transverse strength or bending resistance, which generally involve alterations to the facing component.

3.3.1 Crushing failure load

The crushing axial load, P_u, is calculated by summing the ultimate compressive loads of the facing component and the compressive load of the core component at peak load. A critical calculation factor is the difference in the elasticity modulus between the facing and core components. Typically, the modulus of elasticity for the facing component of FRP-face panels exceeds that of the core. This disparity requires a detailed analysis of the stress experienced by the core component at the strain level where the facing component crushes. Rather than using the ultimate strength of the core component, this stress level is employed for calculations. The approach is justified since the ultimate strength of the core component is theoretical and unlikely to be reached due to panel failure as a result of the crushing of the facing components. In conjunction with the modulus of elasticity for the core component, the ultimate strain of the facing component, ε_{fu},is essential for determining the core component's stress to compute the sandwich panel's axial crushing load capacity, which offers a more accurate alternative to using the core's ultimate strength. Therefore, the equation for the overall sandwich pane's ultimate axial crushing strength is presented as follows:

$$P_u = 2(\sigma_{fu} \cdot t_f \cdot b) + (E_c \cdot \varepsilon_{fu} \cdot t_c \cdot b) \quad (4)$$

3.3.2 Global buckling failure load

Global buckling stems from the panel's slenderness, which may prevent the sandwich panel from achieving the axial crushing failure mode. Traditional analysis often utilizes a simplified critical buckling load, P_{cr}, based on Euler's equation, which integrates the flexural rigidity, *EI*, of the panel:

$$P_{cr} = \frac{\pi^2 \cdot EI}{L^2} \quad (5)$$

where EI is the flexural rigidity defined as:

$$EI = \frac{E_f \cdot t_f{}^3 \cdot b}{6} + \frac{E_f \cdot t_f \cdot b \cdot d^2}{2} + \frac{E_c \cdot b \cdot t_c{}^3}{12} \quad (6)$$

Allen (1969) refined the understanding of buckling in sandwich structures by modifying the Euler equation to better reflect the unique properties of sandwich panels. Allen proposed two distinct formulas based on the thickness ratio of the facing to the overall sandwich thickness:

(a) For thin facings (where the effective depth, d, to thickness of facing, t_f , ratio exceeds 5.77):

$$P_{Global-Thin\ Facings} = \frac{P_E}{1+(P_E/AG)} \quad (7)$$

In this case, the local stiffness of the faces is negligible, allowing the faces to conform to the overall curvature of the beam without significant local deformation. Flexural rigidity is primarily due to the separation of the faces, and the core's shear stiffness plays a significant role in preventing global buckling.

(b) For thick facings (where the effective depth, d, to thickness of facing, t_f , ratio is less than 5.77):

$$P_{Global-Thick\ Facings} = P_E \left[\frac{1+(P_{Ef}/P_c)-(P_{Ef}/P_c) \cdot P_{Ef}/P_E}{1+(P_E/P_c)-(P_{Ef}/P_c)}\right] \quad (8)$$

In the equation, “P_E” is the global Euler buckling load, assuming no core shear strain, calculated as $P_E = \frac{\pi^2 \cdot b \cdot t_f \cdot E_f \cdot d^2}{2 \cdot L^2}$. “$P_{Ef}$” represents the sum of the buckling loads of the facing components, calculated as: $P_{Ef} = \frac{\pi^2 \cdot E_f \cdot I_f}{L^2}$, where “I_f” is s the sum of the second moments of area of the faces about their own centroids and is calculated as $I_f = \frac{b \cdot t_f{}^3}{6}$. “P_c” represents the shear buckling load, calculated as $P_c = A \cdot G_c$, where $A = \frac{b\left(t_c + t_f\right)^2}{t_c}$. For thick faces, the local bending stiffness cannot be ignored. These faces contribute significantly to the overall flexural rigidity of the sandwich panel, resisting bending and deformation more effectively. Here, plane sections may no longer remain plane due to the local bending in the faces, and the shear deformation of the core must be considered.

Similar to the transverse loading, the calculation of the E_f term varies based on whether the sandwich panel is classified as narrow or wide. For narrow panels, E_f corresponds directly to the elastic modulus of the facing material. However, if the panel’s width exceeds the core thickness—a typical scenario for walls—then E_f is recalculated as $\frac{E_f}{(1-\nu_f{}^2)}$. If the wide panel is assumed to bend cylindrically, this adjustment applies. If it is assumed to bend anticlastic, then E_f remains unchanged.

3.3.3 Local buckling failure load

Local buckling, which often appears as wrinkling in the face sheets of sandwich panels, is a critical failure mode that may occur before global buckling or crushing failure modes under certain conditions. This failure typically results from excessive compressive stresses that exceed the stability threshold of the face sheet, influenced significantly by its interaction with the core. Predicting the onset of local buckling entails developing a model that treats the face sheet as a beam on an elastic foundation. As outlined in Allen (1969), this approach effectively captures the complex interactions between the flexible face sheet and the supportive core, which are fundamental for the initiation of wrinkling. However, the approach is based on an unknown critical length that is solved iteratively. Noël and Fam (2021) applied the approach to a large set of experimental data and proposed the following empirical equation for the critical local buckling load, P_{Local}:

$$P_{Local} = t_c \cdot \sqrt{t_f} \cdot b \cdot \left(\frac{E_c}{(3-\nu_c)\cdot(1+\nu_c)}\right)^{2/3} \tag{9}$$

In which, ν_c, represents the Poisson's ratio of the core material, which quantifies the ratio of transverse strain to axial strain and is crucial for understanding how the core deforms under compressive stresses. It should be noted that Equation 9 was rearranged based on multiple equations proposed by Noël and Fam (2021).

4. ENGINEERING AND TESTING FOR SIP COMPLIANCE

In the absence of a Canadian standard regarding testing procedures for SIPs, this section highlights the established testing methodologies widely recognized in academic literature and commonly requested by building officials in Canada. The goal is to validate the load-bearing capabilities of SIPs, a process that often entails third-party evaluations. These important appraisals ensure SIPs can withstand designated loads—a requirement enforced by numerous building authorities.

In contrast, the United States has adopted AC04 as the recognized standard for SIP testing. AC04 encompasses detailed protocols for assessing the structural and thermal performance of SIPs, providing a comprehensive framework that ensures compliance with building codes. This standard is instrumental in guiding manufacturers and builders in the U.S. to achieve verified levels of safety and performance.

4.1 Structural Performance Testing

Without specific SIP testing standards within the Canadian Standards Association (CSA), building officials in Canada often recommend the AC04. This recommendation ensures that despite the lack of localized testing criteria, SIPs undergo a thorough evaluation based on AC04's rigorous benchmarks. The approach was effectively demonstrated in the work conducted by Abbasi and Sennah (2013), where research focused on two critical assessments: compressive testing to evaluate vertical load-bearing capacity, and transverse (four-point bending) testing to assess the panels' flexural capacity. Conducted within the context of residential construction, this analysis ensures that SIP construction meets or exceeds the established benchmarks for strength and deflection, aligning with the expectations set for traditional wood-frame constructions.

Furthermore, racking tests are crucial for evaluating the strength of SIPs against lateral forces from wind and seismic events, essential for designing shear walls. Research by Terentiuk and Memari (2012) demonstrates that SIPs can exceed expected performance metrics under both monotonic and cyclic loading conditions. These large-scale tests, which simulate real-life scenarios, show that SIPs can effectively manage drifts beyond 127 mm (5.00 inches; 5.2% drift ratio), surpassing the maximum allowable drift ratio of 2.5% as defined by the American Society of Civil Engineers (ASCE) 7-05 (ASCE, 2006).

4.2 Deflection and Flexural Creep Behavior

Understanding deflection limits is critical, particularly any parameters stemming from immediate loads like dead and live loads. These limits often serve as primary design benchmarks. It is equally important, however, to account for the susceptibility of non-metallic SIPs to undergo creep—a phenomenon that can lead to deflections exceeding initial estimates over time due to the material's response to sustained loads. This requires a shift towards a greater comprehensive design approach that incorporates long-term deflection. Acknowledging this need, the study conducted by Taylor et al. (1997) becomes particularly relevant. Their research focuses on the flexural creep deflection of SIPs made from OSB and foam, offering valuable insight into the long-term effects of sustained loads on SIP structures. By applying various viscoelastic models, the work predicts relative creep deflections of SIPs, emphasizing the need for integrating creep behaviour into both the design and evaluation processes.

In addition to addressing creep behavior, ensuring the structural integrity and performance of SIPs over time requires airtightness testing of panel connections. This testing, which can be conducted in accordance with ASTM E2357, is essential for verifying the airtightness of the panel joints, a critical factor in maintaining thermal efficiency and structural durability under operational conditions. Therefore, new forms of SIP—especially those fabricated from non-traditional materials—must undergo long-term testing aligned with ASTM C480 standards. A pivotal process outcome is the determination of a “creep coefficient” or “K_{cr}.” This coefficient is important for refining deflection predictions, using the equation $\Delta_T = K_{cr} \cdot \Delta_{LT} + \Delta_{ST}$ where Δ_T represents the total deflection, Δ_{LT}, is the deflection due to long-term sustained load and Δ_{ST} is deflection due to transient load.

4.3 Panel Connections and System Performance

Panel connections play a key role in the overall performance of SIP systems, affecting aspects like thermal resistance, vulnerability to pests, airtightness, and structural integrity (SIPA, 2008). These connections include the surface spline or OSB thin spline, depicted in Figure 4(a), which uses OSB to create a seamless connection, significantly reducing thermal bridging. Another connection type is block spline or foam block spline, designed to enhance joint strength and simplify the assembly process, as demonstrated in Figure 4(b). Additionally, the double dimensional lumber spline—illustrated in Figure 4(c)—is tailored to applications requiring higher load-bearing capacity, though it requires meticulous sealing to mitigate thermal bridging (Rungthonkit, 2012; Morley, 2000; SIPA, 2008). These connections are informed by a comprehensive understanding of each type's functionality within the system. This approach is supported by the research of Du et al. (2021), which explores the thermal performance of SIP splines through experimental measurement and finite element analysis, focusing on the effects of material properties, insulation thickness, and nail configurations on thermal transmittance. Notably, thermal transmittance increases by 11.9%, 10%, and 60% for surface, block, and double 38 mm × 140 mm splines, respectively, compared to unconnected panels (Du et al., 2021). These findings underscore the necessity of evaluating SIP connections for both thermal efficiency and bonding strength.

4.4 Design Tables

Design tables are invaluable for commercializing non-traditional SIP or their incorporation into future projects, offering detailed information on their performance under various load conditions. Compiling these tables involves analyzing their responses to combinations of dead, live, and snow loads in line with established guidelines within the NBCC. The tables note predefined panel dimensions, structural capacities, and optimal joist spans, serving as an essential guide for effectively designing with non-traditional SIPs. Furthermore, they ensure safe designs are compliant with code strength requirements. In summary, the full process of designing FRP-faced SIPs, from initial analysis to compliance with building codes and final testing, is encapsulated in the flowchart shown in Figure 5.

5. DESIGN EXAMPLE: FRP-FACED SIPs

Amidst the renovation of a culinary establishment's kitchen—designed to cater to both high-heat cooking and precision cooling needed for cake decoration—the owner chooses to explore FRP-faced SIPs over traditional construction methodologies. This decision is rooted in the superior thermal insulation properties of SIPs, which promise significant operational efficiencies and potential reductions in annual heating and cooling expenditures. The project delineates a FRP-faced SIP application tailored for the kitchen floor and wall systems located on the ground floor of a two-storey building in Halifax, Nova Scotia, Canada. The proposed FRP-faced SIP incorporates advanced materials, including GFRP facings and a PE foam core, with a density of 80 kg/m^3. The design takes into account how flooring will not be attached to any non-structural elements vulnerable to damage from significant deflections. The following specifications are provided:

- GFRP facing: each ply has a thickness of 1.02 mm, Poisson’s ratio of 0.3, with a tensile strength of 621 MPa, elastic modulus of 37 GPa, and an average ultimate strain of 0.0168 mm/mm.
- PE foam core: This newer generation material, specifically designed for structural applications, features a density of 80 kg/m^3, elastic modulus of 24 MPa, Poisson’s ratio of 0.3, shear modulus of 10.5 MPa, shear strength of 0.66 MPa, and thermal conductivity of 0.167 BTU in/ft^2 hr °F. The properties and conductivity values are based on manufacturer specifications from ResTex Composites (ResTex Composites, 2023).

Importantly, the design uses innovative materials, therefore the final design obtained through this solution must undergo comprehensive large-scale testing to verify the strength and durability of the panels. Such testing is crucial to potentially reveal premature failures, impacting the structural integrity and overall suitability for construction. Figure 6 illustrates a simplified schematic of the proposed wall and roof configuration, which illustrates the placement and dimensions of the SIP panels.

5.1 Floor: Preliminary design solution

Considering the commercial setting of the kitchen, the design complies with the NBCC's standard service live load requirement of 4.8 kPa. The total estimated dead load for the commercial kitchen is approximately 1.8 kPa. This includes about 0.3 kPa from the SIPs, assuming their final design features a 300mm thickness. Additionally, the weight from drop ceilings and finishes contributes about 0.052 kPa. Utilities—encompassing plumbing, electrical systems, and Heating, ventilation, and air conditioning (HVAC)—add an additional 0.4 kPa. Completing this load are the permanent fixtures and heavy appliances typical in commercial kitchens, contributing around 1.0 kPa.

The SIP floor is designed with simple support conditions across a span of seven meters. To ensure compliance with these conditions in practical applications, each end of the SIP is supported by a continuous bearing that is determined by the specific requirements of the project, typically extending a minimum of 76 mm (approximatly three inches). This configuration is essential for maintaining structural integrity and aligns with industry-standard practices (Thermapan Structural Insulated Panels, Inc., 2023). As shown in Figure 6, the SIP floor is connected to the exterior wall, which implicates specific thermal insulation requirements. It is important to distinguish between floors between different levels, which do not connect to the exterior and therefore have no thermal insulation requirements, and floors that do connect or form part of the exterior envelope, as in this case. For this SIP connected to the exterior, the initial analysis phase involves determining the thickness of the core material to meet thermal insulation requirements mandated by the NECB for

Zone 6 (located in Halifax, Nova Scotia, Canada). The code specifies a maximum thermal transmission rate for floors as 0.156 W/m^2K. Subsequently, to calculate the minimum core thickness necessary for adequate thermal insulation, the following equation is applied:

$$\text{Core Thickness (m)} = \frac{0.167\ \text{BTU in}}{\text{ft}^2\ \text{hr}\ °\text{F}} \cdot \frac{0.144\ \text{W/mK}}{1\text{BTU in/ft}^2\ \text{hr}\ °\text{F}} \cdot \frac{1}{0.156\text{W/m}^2\text{K}} = 0.154\ \text{m or } 154\ \text{mm}$$

This equation derives from converting the BTU value (a measure of thermal resistance) to a corresponding value in watts per meter-kelvin (W/mK), reflecting the material's thermal conductivity. The conversion factor of 0.144 W/mK to 1 BTU in/ft^2 hr °F is used to align the units across units across different standard measurements, ensuring the equation's relevance to the NECB's requirements. Given the design's emphasis on thermal insulation, the core thickness is adjusted to 200 mm. Consequently, the design progresses to determine the necessary number of GFRP ply layers for the facings, noting that each ply measures 1.02 mm. This approach is rooted in the practicalities of manufacturing, ensuring that design aligns with feasible fabrication techniques. This step considers three potential failure modes of sandwich panels under transverse loading: face rupture, wrinkling, and core shear. Specific equations (Equations 1, 2, and 3) analyze these failure modes for a 1-meter section of flooring to determine the minimum required thickness of GFRP facings, identifying the optimal number of ply layers necessary for adequate load-bearing capacity. The analysis extends to graphical representations, plotting the distributed load per unit width (1000 mm) against the number of GFRP layers in the facing, as shown in Figure 7. This helps quantify how variations in layer count influence the panel's structural performance. Further calculations employ the allowable stress design (ASD) method with a safety factor of three to determine the distributed factored load as follows:

$$\text{Factored Load} = (\underbrace{4.8\ \text{kN/m}^2}_{\text{Live load}} + \underbrace{1.8\ \text{kN/m}^2}_{\text{Dead load}}) \times \underbrace{3}_{\text{Safety factor}} \cong 20\ \text{kN/m}$$

The calculation results in a distributed factored load of 20 kPa, equivalent to 20 N/mm for a 1-meter strip of flooring. As indicated in Figure 7, at a configuration of 6 GFRP ply layers, the factored load resisted by the panel exceeds 20 N/mm, which is the design load. At this juncture, the primary failure mode is wrinkling of the facing component. This suggests that the substantial thickness of the core intended to meet the thermal insulation requirements concurrently enhances the panels' ability to withstand higher loads without core shear dominating as a failure mode. Hence, the GFRP facings must have at least 6 GFRP ply layers per facing. This requirement ensures compliance with thermal insulation standards and effectively addresses the strength requirements under the ASD method.

To further validate these findings, a quick checkpoint using the equation derived from Allen's principles can be implemented. This will confirm the assumption that the facings predominantly bear the bending stresses while the core's shear stress is simplified to a constant value. The specific inequality to check is:

$$4 \cdot \frac{E_f}{E_c} \cdot \frac{t_f}{t_c} \cdot \frac{d}{t_c} > 100$$

Substituting the given values:

$$4 \cdot \frac{37000 \text{ MPa}}{24 \text{ MPa}} \cdot \frac{(6 \times 1.02)\text{mm}}{154 \text{ mm}} \cdot \frac{154 \text{ mm} + (6 \times 1.02)\text{mm}}{154 \text{ mm}} = 254.8 > 100$$

This validation reinforces the design approach and assumptions regarding load distribution between the facings and the core.

For assessing the total deflection against code-prescribed limits, the following equation—incorporating both bending and shear deflection components—is used to calculate the total deflection. Since the panel is assumed to be wide (i.e., the width b is much larger than the core thickness t_c), E_f is adjusted using the Poisson's ratio, ν_f . Specifically, E_f is replaced with $\frac{E_f}{1-\nu_f^2}$:

$$\Delta_T = \Delta_B + \Delta_S = \frac{5 \cdot \mathrm{w} \cdot \mathrm{L}^4 \cdot (1 - v_f^2)}{192 \cdot \mathrm{b} \cdot \mathrm{d}^2 \cdot \mathrm{t_f} \cdot \mathrm{E_f}} + \frac{\mathrm{w} \cdot \mathrm{L}^2 \cdot \mathrm{t_c}}{8 \cdot \mathrm{b} \cdot \mathrm{d}^2 \cdot \mathrm{G}} = \frac{5 \cdot (4.8) \cdot (7000^4) \cdot (1 - 0.3^2)}{192 \cdot (1000) \cdot (208^2) \cdot (6.12) \cdot (37000)} + \frac{(4.8) \cdot (7000^2) \cdot (200)}{8 \cdot (1000) \cdot (208^2) \cdot (10.5)} \cong 41 \text{ mm}$$

The calculation indicated a deflection of 41 mm, exceeding the allowable limit of:

$$\Delta_{Allowable} = \frac{L}{360} = \frac{7000}{360} = 19.4 \text{ mm}$$

In response to exceeding the deflection criteria, modifications were made by adding three additional plies of GFRP per facing and simultaneously increasing the core depth to 300 mm.

$$\Delta_T = \Delta_B + \Delta_S = \frac{5 \cdot w \cdot L^4 \cdot (1 - v_f^2)}{192 \cdot b \cdot d^2 \cdot t_f \cdot E_f} + \frac{w \cdot L^2 \cdot t_c}{8 \cdot b \cdot d^2 \cdot G} = \frac{5 \cdot (4.8) \cdot (7000^4)(1 - 0.3^2)}{192 \cdot (1000) \cdot (309^2) \cdot (9) \cdot (37000)} + \frac{(4.8) \cdot (7000^2) \cdot (300)}{8 \cdot (1000) \cdot (309^2) \cdot (10.5)} = 17.4 \text{ mm}$$

These adjustments reduced the total deflection to 17.4 mm, thereby aligning with the acceptable deflection limit and illustrating the efficacy of these enhancements in meeting structural requirements. Consequently, the optimal solution for the floor construction requires an SIP with a thickness of 300 mm, and nine layers of GFRP ply on each facing to ensure both structural integrity and compliance with thermal insulation standards.

5.2 Wall: Preliminary design solution

The wall design pertains to an exterior wall with an unsupported height of 3m. Each segment of this exterior wall is designed to be completely enclosed, containing no openings for windows or doors, which enhances its structural integrity and thermal insulation capabilities. The initial step involves addressing thermal insulation requirements as outlined by the NECB for Zone 6 (Halifax). This zone mandates a maximum thermal transmission rate of 0.24 W/m^{2}K for walls. To meet these thermal insulation criteria, the equation applied leads to a minimum core thickness of 100 mm:

$$\text{Core Thickness} = \frac{0.167 \text{ BTU in}}{\text{ft}^2 \text{ hr °F}} \cdot \frac{0.144 \text{ W/mK}}{1\text{BTU in/ft}^2 \text{ hr °F}} \cdot \frac{1}{0.24 \text{ W/m}^2\text{K}} = 0.100 \text{ m or } 100 \text{ mm}$$

This calculation confirms that a core thickness of at least 100 mm is required to fulfill the thermal insulation criteria for the walls. The subsequent structural analysis incorporates not only the dead and live loads typically considered for a ground-level wall but also the additional live load from the roof and snow load, which are critical given the geographic location. According to the NBCC, the roof live load is specified at 1.0 kN/m², and the snow load is set at 1.9 kN/m² for Halifax.

The structural requirements—specifically the number of GFRP ply layers required for facings to resist axial loads—consider a tributary area of 3.5 meters by 0.5 meters, with each ply measuring 1.02 mm in thickness. The structural analysis considers four critical failure modes for the sandwich panels under axial loading: face crushing, global buckling using Euler's equation, global buckling using Allen's equation, and local buckling. These modes are evaluated using Equations 4, 5, 7, and 9 to determine the minimal thickness of GFRP facings required to efficiently support loads. Equation 7, rather than Equation 9, was used for global buckling according to Allen's equation because the panel is assumed to have a thin facing, where the effective depth, d, to thickness of facing, t_f, ratio is assumed to be more than 5.77. This assumption needs to be verified after determining the thickness of the facing component. Figure 8 depicts these evaluations, illustrating how the load per unit width varies with the number of GFRP layers.

Using the ASD method with a safety factor of three, the distributed factored surface load was calculated by combining the dead loads, live load from the floor above the kitchen, and the maximum of the live or snow load from the roof:

$$\left(\underbrace{4.8\ \mathrm{kN/m^2}}_{\text{Floor live load}} + \max\left(\underbrace{1\ \mathrm{kN/m^2}}_{\text{Roof live load}}, \underbrace{1.9\ \mathrm{kN/m^2}}_{\text{Roof snow load}}\right) + \left(\underbrace{1.8\frac{\mathrm{kN}}{\mathrm{m^2}}}_{\text{Dead load}} \times \underbrace{2}_{\text{Floor+roof}}\right)\right) \times \underbrace{3}_{\text{Safety factor}} \cong 31\ \mathrm{kN/m^2}$$

Multiplying the calculated distributed load by the tributary width that the exterior wall supports, the total load that the wall must support from the roof and floor is:

$$31\ \mathrm{kN/m^2} \times \underbrace{3.5\ \mathrm{m}}_{\text{Tributary width}} \cong 109\ \mathrm{kN/m}$$

Additionally, the load calculations must include the weight from the walls and the parapet, as depicted in Figure 6. The SIP weighs 0.1 kPa when 100 mm thick, with the exterior cladding approximately 0.6 kPa and the interior drywall around 0.3 kPa, resulting in a total load of approximately 1 kPa. Multiplying this by the height of the wall (3 m), the wall above (3 m), and the parapet (1 m), and applying a safety factor of 3, the total load from the walls and parapet is calculated as follows:

$$\left(\underbrace{0.1\ \mathrm{kN/m^2}}_{\text{SIP load}} + \underbrace{0.6\ \mathrm{kN/m^2}}_{\text{Cladding load}} + \underbrace{0.3\ \mathrm{kN/m^2}}_{\text{Drywall load}}\right) \times \underbrace{(3\ \mathrm{m} + 3\ \mathrm{m} + 1\ \mathrm{m})}_{\text{Height of walls and parapet}} \times \underbrace{3}_{\text{Safety factor}} = 21\ \mathrm{kN/m}$$

Adding those two loads we get that the wall shall support 130 kN/m. This calculated factored load of 130 kN/m indicates that global buckling is the predominant failure mode under the specified axial loading conditions. The graphical analysis in Figure 8 suggests that although 0.7 GFRP ply layers per facing would suffice, fractional layers cannot be requested from the manufacturer. Therefore, at least 1 full ply is required to adequately support this load. Consequently, the solution for the wall design to successfully resist the applied axial loads and meet the thermal insulation criteria includes a core thickness of 100 mm with 1 GFRP ply layer per facing. A final check is conducted to ensure the panel is indeed thin-faced, confirming the proper application of Allen's global buckling equation. The ratio of effective depth to facing thickness, calculated as 99, is significantly greater than 5.77, thereby validating the design.

6. CONCLUDING REMARKS

This paper investigates the use of FRP-faced SIPs across various applications within the construction industry in both the United States and Canada, focusing on their use in floors, walls, and roofs. It highlights a significant gap in the NBCC regarding the lack of comprehensive design guidelines for SIPs, emphasizing the need for developing compliance strategies that integrate both established and innovative approaches tailored to improve the structural and thermal performance of FRP-faced SIPs. By developing a design framework based on the principles of materials mechanics, the paper aims to enhance FRP-faced SIP configurations to increase thermal insulation and structural performance. This framework is supported by empirical testing methodologies derived from established literature, providing a guide for new builders in the absence of specific governmental documentation and clarifying the necessary testing protocols to validate SIP designs.

The paper offers insights into designing SIP components subjected to various loading conditions, such as transverse loads for roofs and floors, and axial loads for wall components. A detailed design example is provided to illustrate the application of these methodologies. Through this analysis, the paper strives to bridge the existing regulatory and knowledge gaps, facilitating a deeper understanding and more effective use of FRP-faced SIPs in the construction sector. The design examples demonstrate the potential of FRP-faced SIPs in enhancing both thermal and structural performance.

In addition to the aspects covered in this paper, it is recommended for future studies to explore the differences in required dimensions and costs between traditional OSB-based panels and innovative FRP-faced SIPs. Such comparisons will aim to quantify the cost-effectiveness and dimensional suitability of using advanced materials in construction practices, further contributing to the development of optimized building solutions. Furthermore, in light of upcoming changes in Canadian codes, it is critical for future research to include life cycle assessment (LCA) analysis to evaluate the embodied carbon emissions of SIPs. Additionally, assessing the durability and long-term performance of FRP materials through methods such as accelerated aging and field monitoring will be imperative. This will ensure that future applications of FRP-faced SIPs not only meet current performance standards but also withstand environmental degradation factors.

NOTATION LIST

The following symbols are used in this paper:

A = cross-sectional area;

$A \cdot G$ = shear stiffness;

b = width of the sandwich panel;

E_c = core's modulus;

E_f = facing's modulus of elasticity;

EI = flexural rigidity;

F = tension or compression force resisted by the facing during bending;

G_c = core's shear modulus;

I_f = sum of the second moments of area of the faces about their centroids;

K_{cr} = creep coefficient;

L = span length;

M = bending moment;

P_c = shear buckling load;

P_{cr} = critical buckling load;

P_{Ef} = sum of the buckling loads of the facing components;

P_E = global Euler buckling load;

P_u = crushing axial load;

t_c = core thickness;

t_f = facing thickness;

V = shear force;

w = uniformly distributed factored load;

w_{CS} = ultimate distributed load that can induce core shear failure;

w_{FR} = = ultimate distributed load that could induce face rupture;

w_{WR} = ultimate distributed load that could induce wrinkling failure;

Δ_B = bending deflection;

Δ_{LT} = deflection due to long-term sustained load;

Δ_S = shear deflection;

Δ_{ST} = deflection due to transient load;

Δ_T = total deflection;

ε_{fu} = ultimate strain of the facing component;

σ_{fu} = rupture stress in the facing;

σ_{WR} = stress causing wrinkling;

τ_c = core's shear stress;

ν_C = Poisson's ratio of the core material;

ν_f = Poisson's ratio of the facing material.

REFERENCES

Abbasi, H., & Sennah, K. (2013). Comparative Structural Behavior of Insulated Sandwich Foam-OSB Walls and Floor with Conventional Timber Stud Panels in Residential Buildings. In Proceedings of the 3rd Specialty Conference on Material Engineering & Applied Mechanics, May 29 to June 1, Montréal, Québec.

Allen, H. G. (2013). Analysis and design of structural sandwich panels: the commonwealth and international library: structures and solid body mechanics division. Elsevier.

Amran, Y. H. M., El-Zeadani, M., Lee, Y. H., Lee, Y. Y., Murali, G., & Feduik, R. (2020). Design innovation, efficiency and applications of structural insulated panels: A review. Structures, 27, 1358-1379. https://doi.org/10.1016/j.istruc.2020.07.044.

ASCE. (2006). "Minimum design loads for buildings and other structures." ASCE 7-05, Reston, Virginia.

ASTM International. (2016). ASTM C480/C480M-16, Standard Test Method for Flexure Creep of Sandwich Constructions. https://www.astm.org

ASTM International. (2022). D198 - 22 Standard Test Methods of Static Tests of Lumber in Structural Sizes. ASTM International. https://www.astm.org/d0198-22.html.

ASTM International. (2018). ASTM E2357-18, Standard test method for determining air leakage rate of air barrier assemblies. ASTM International. https://www.astm.org

Betts, D., Sadeghian, P., & Fam, A. (2018). Experimental behavior and design-oriented analysis of sandwich beams with bio-based composite facings and foam cores. Journal of Composites for construction, 22(4), 04018020.

Canadian Commission on Building and Fire Codes. (2022). National Building Code of Canada: 2020. National Research Council of Canada. https://doi.org/10.4224/w324-hv93

Canadian Commission on Building and Fire Codes. (2022). National Energy Code of Canada for Buildings: 2020. National Research Council of Canada. https://doi.org/10.4224/rr3q-hm83

CoDyre, L., & Fam, A. (2017). Axial strength of sandwich panels of different lengths with natural flax-fiber composite skins and different foam-core densities. Journal of Composites for Construction, 21(5), 04017042.

Drain, D., Chiang, J., Mewis, B., & Duggan, T. (2006). Time & Motion Study. Reed Construction Data/RSMeans. BASF Corporation. [Submitted to BuildingInsight, LLC. - Christopher J. Fennell, President]. Reed Construction Data, Inc.

Du, Q., Jin, L., Lv, J., Cai, C., & Zhang, R. (2021). Experimental and numerical studies on the thermal performance of structural insulated panel splines. Journal of Building Engineering, 44, 103334. https://doi.org/10.1016/j.jobe.2021.103334

Fact.MR. (2023, May 16). Structural Insulated Panels Market Size to Record Exponential Growth at a CAGR of 5.1% by 2033: Fact.MR Report. https://www.factmr.com/connectus/sample?flag=S&rep_id=6628

Fam, A., & Sharaf, T. (2010). Flexural performance of sandwich panels comprising polyurethane core and GFRP skins and ribs of various configurations. Composite Structures, 92(12), 2927-2935.

Fu, Y., & Sadeghian, P. (2023). Bio-based sandwich beams made of paper honeycomb cores and flax FRP facings: Flexural and shear characteristics. Structures, 54, 446-460. https://doi.org/10.1016/j.istruc.2023.05.064

Fu, Y., & Sadeghian, P. (2020). Flexural and shear characteristics of bio-based sandwich beams made of hollow and foam-filled paper honeycomb cores and flax fiber composite skins. Thin-Walled Structures, 106834. https://doi.org/10.1016/j.tws.2020.106834

Garrido, M., & Correia, J. R. (2018). Elastic and viscoelastic behaviour of sandwich panels with glass-fibre reinforced polymer faces and polyethylene terephthalate foam core. Journal of Sandwich Structures & Materials, 20(4), 399-424.

Hristozov, D., Wroblewski, L., & Sadeghian, P. (2016). Long-term tensile properties of natural fibre-reinforced polymer composites: Comparison of flax and glass fibres. Composites Part B: Engineering, 95, 82-95.

International Code Council. (2023). 2024 International Building Code (IBC).

International Code Council. (2017). 2018 International Energy Conservation Code (IECC).

International Code Council. (2021). 2021 International Residential Code (IRC).

ICC Evaluation Service. (2020). Acceptance criteria for sandwich panels (AC04) (Editorially revised December 2020). https://icc-es.org/acceptance-criteria/ac04/

IECC Evaluation Service. (2020). Acceptance criteria for sandwich panels (AC04) (Editorially revised December 2020). https://icc-es.org/acceptance-criteria/ac04/

Kassab, R., & Sadeghian, P. (2023, August). Effects of material non-linearity on the structural performance of sandwich beams made of recycled PET foam core and PET fiber composite facings: Experimental and analytical studies. In Structures (Vol. 54, pp. 1259-1277). Elsevier.

Kassab, R., & Sadeghian, P. (2023, November). Impact of the bio content of polymeric matrices on flexural performance of sandwich beams made of PET fiber composite facings and recycled PET honeycomb core. In Structures (Vol. 57, p. 105057). Elsevier.

Kelley, S. P., & Blanford, M. (2023). Concept of thermal bridging in wood framed construction. Cityscape, 25(1), 315-321. U.S. Department of Housing and Urban Development. https://www.jstor.org/stable/48725048.

Koones, S. (2013). Prefabulous+ sustainable: Building and customizing an affordable, energy-efficient home. Abrams.

Manalo, A., Aravinthan, T., Fam, A., & Benmokrane, B. (2017). State-of-the-art review on FRP sandwich systems for lightweight civil infrastructure. Journal of Composites for Construction, 21(1), 04016068.

McCracken, A., & Sadeghian, P. (2018). Corrugated cardboard core sandwich beams with bio-based flax fiber composite skins. Journal of Building Engineering, 20, 114-122. https://doi.org/10.1016/j.jobe.2018.07.009

McCullom, I, & Krarti, M. "A Simple Method to Estimate Energy Savings for Structural Insulated Panels Applied to Single Family Homes." Proceedings of the ASME 2010 4th International Conference on Energy Sustainability. ASME 2010 4th International Conference on Energy Sustainability, Volume 2. Phoenix, Arizona, USA. May 17–22, 2010. pp. 357-362. ASME. https://doi.org/10.1115/ES2010-90353

Mostafa, A., Shankar, K., & Morozov, E. V. (2014). Experimental, theoretical and numerical investigation of the flexural behaviour of the composite sandwich panels with PVC foam core. Applied Composite Materials, 21(4), 661-675.

Moynihan, A. E. (2014). Evaluating the Benefits of and Barriers to Building with Structural Insulated Panels. Student Showcase, 5. University of Massachusetts Amherst. Retrieved from https://scholarworks.umass.edu/sustainableumass_studentshowcase/5.

Noël, M., & Fam, A. (2021). Empirical Design Equation for Compression Strength of Lightweight FRP Sandwich Panel Walls. Journal of Architectural Engineering, 27(3), 04021029.

NTA, Inc. (2009). Engineered Design of SIP Panels Using NTA Listing Report Data (IM 14 TIP 01). Nappanee, Indiana: Author.

Panjehpour, M., Abang Ali, A. A., & Voo, Y. L. (2013). Structural insulated panels: Past, present, and future. Journal of Engineering, Project, and Production Management, 3(1), 2-8.

Reis, E. M., & Rizkalla, S. H. (2008). Material characteristics of 3-D FRP sandwich panels. Construction and Building Materials, 22(6), 1009-1018.

ResTex Composites. (2023). PE foam core product specifications. Retrieved from https://www.mcssl.com/store/restexcomposites/core-material/pe-foam. Rungthonkit, P. (2012). Structural behaviour of structural insulated panels (SIPS) [Doctoral dissertation, University of Birmingham]. University of Birmingham eTheses Repository. http://etheses.bham.ac.uk/id/eprint/3561

Structural Insulated Panel Association. (2008). BEST Building Education with SIPs Training – Basic SIP Design and Engineering. Retrieved from www.sips.org

Taylor, S. B., Manbeck, H. B., Janowiak, J. J., & Hiltunen, D. R. (1997). Modeling structural insulated panel (SIP) flexural creep deflection. Journal of Structural Engineering, 123(12), 1658-1665. American Society of Civil Engineers.

Terentiuk, S., & Memari, A. (2012). In-Plane Monotonic and Cyclic Racking Load Testing of Structural Insulated Panels. Journal of Architectural Engineering, 18(4), 261-275. https://doi.org/10.1061/(ASCE)AE.1943-5568.0000084.

Thakur, V. K., Thakur, M. K., & Kessler, M. R. (Eds.). (2017). Handbook of Composites from Renewable Materials, Design and Manufacturing. John Wiley & Sons.

Thermapan Structural Insulated Panels, Inc. (2023). Design handbook: Load & span table for SIP designers; Exterior walls, foundations walls, roofs, and floors. Fort Erie, Ontario, Canada: Author.

Xie, H., Shen, C., Fang, H., Han, J., & Cai, W. (2022). Flexural property evaluation of web reinforced GFRP-PET foam sandwich panel: Experimental study and numerical simulation. Composites Part B: Engineering, 234, 109725.

Yang, J., & Rungthonkit, P. (2009). Behaviour of structural insulated panels (SIPs) under both short-term and long-term loadings. 11th International Conference for Non-conventional Materials and Technologies: Materials for Sustainable and Affordable Construction, September 6, 2009. University of Birmingham Research Portal. https://research.birmingham.ac.uk/en/publications/behaviour-of-structural-insulated-panels-sips-under-both-short-te

Zenkert, D. (1997). The Handbook of Sandwich Construction. Engineering Materials Advisory Services.

Zhou, T., Zhang, P., Xiao, W., Liu, J., & Cheng, Y. (2019). Experimental investigation on the performance of PVC foam core sandwich panels under air blast loading. Composite Structures, 226, 111081.

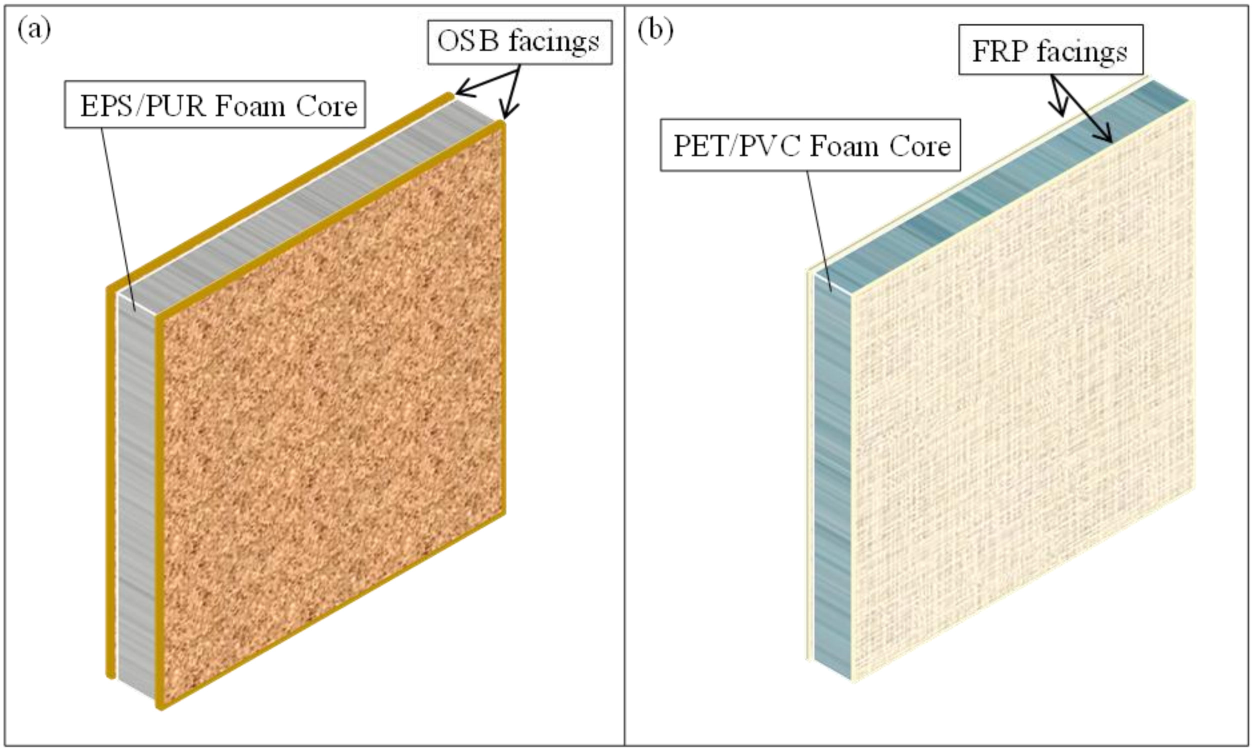

Figure 1: A 3D illustration depicting the cross-section of a simplified SIP, with annotations highlighting its core and facing elements: (a) showcases a traditional panel with a thicker OSB facing; and (b) displays a non-traditional panel distinguished by a thinner FRP facing.

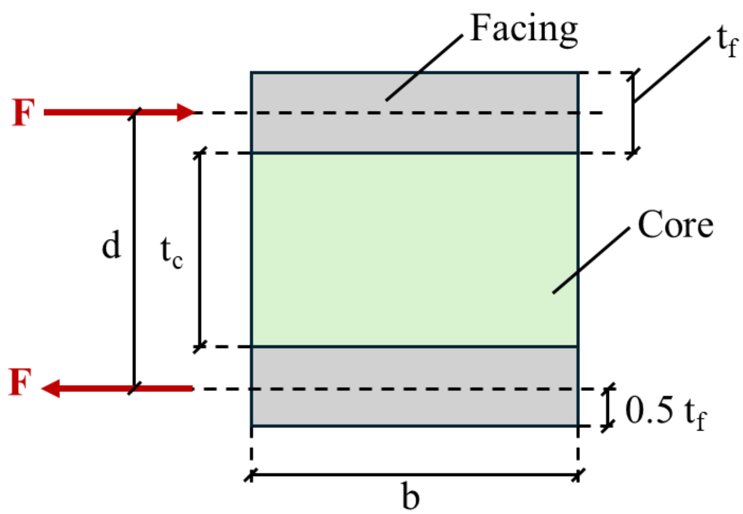

Figure 2: Cross-section of a sandwich panel illustrating its components and their dimensions.

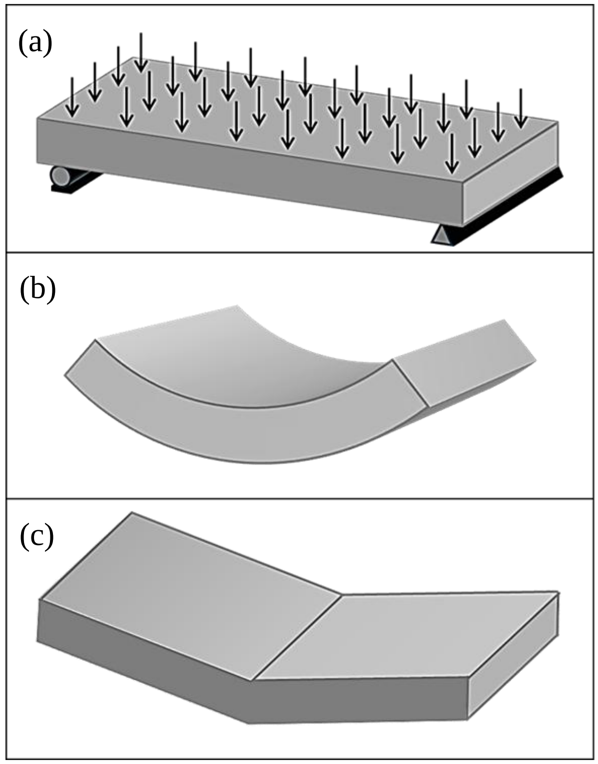

Figure 3: Analysis of SIP deflections: (a) illustrates a uniformly distributed load applied to a SIP in a simply supported condition; (b) depicts bending deflection; and (c) shear deflection.

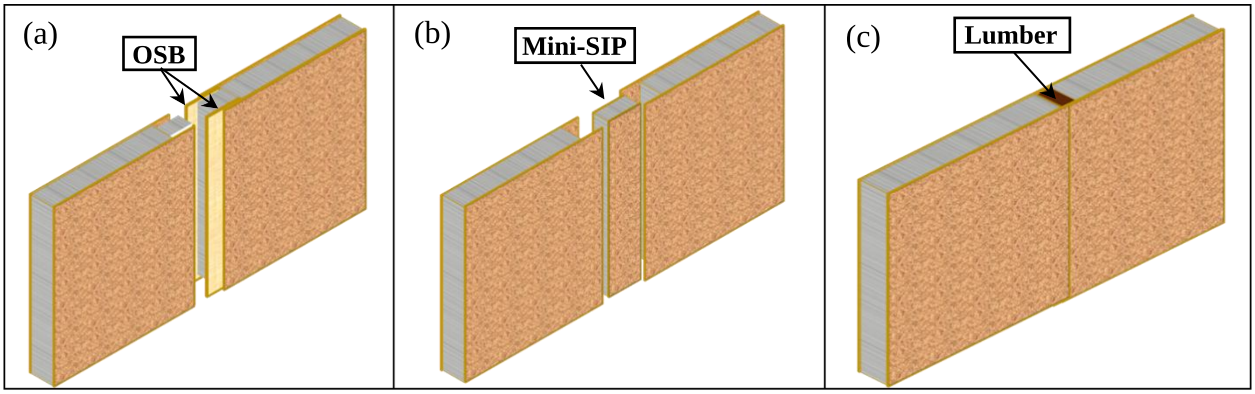

Figure 4: 3D Views of SIP connection techniques: (a) surface spline, or OSB thin spline; (b) block spline, also known as foam block spline or mini-SIP; (c) dimensional lumber spline, with a single lumber detail shown.

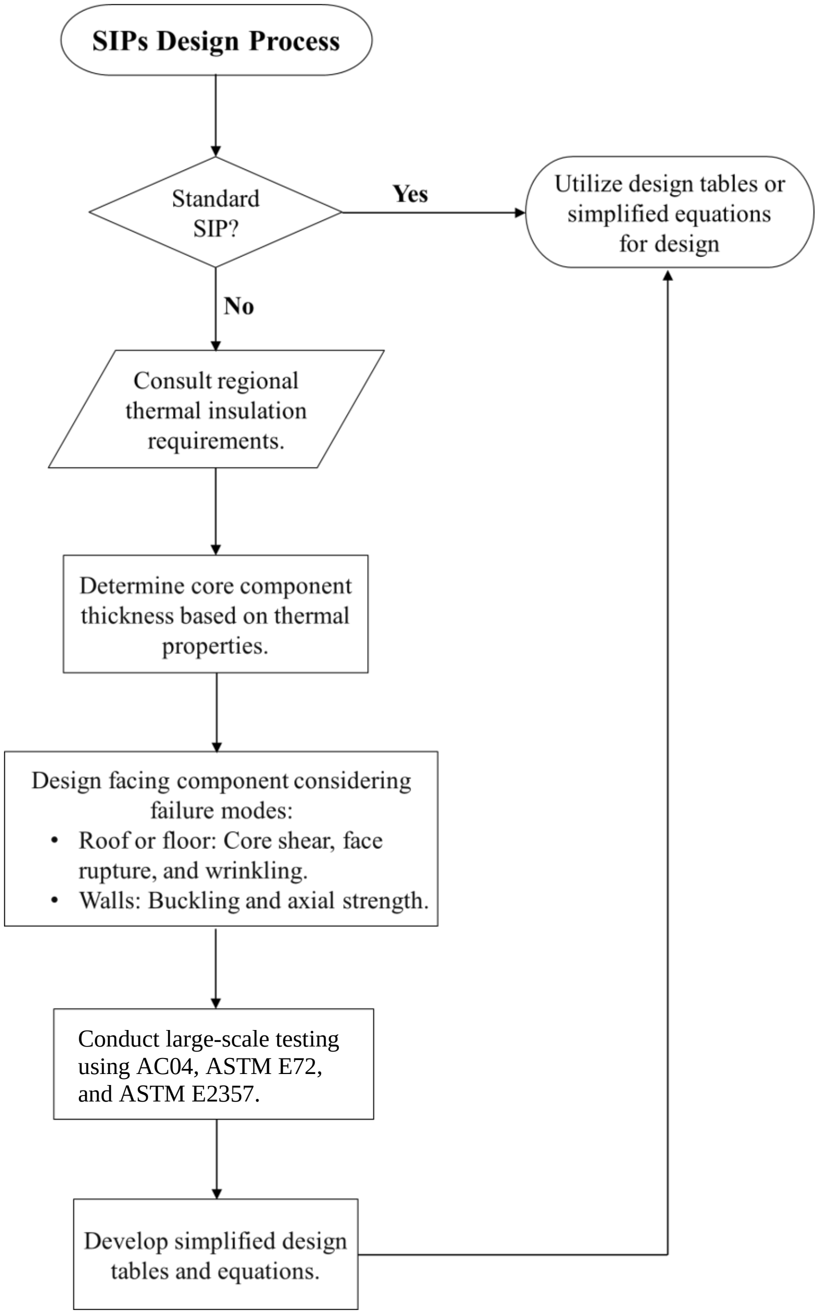

Figure 5: Flowchart depicting the design process of SIPs.

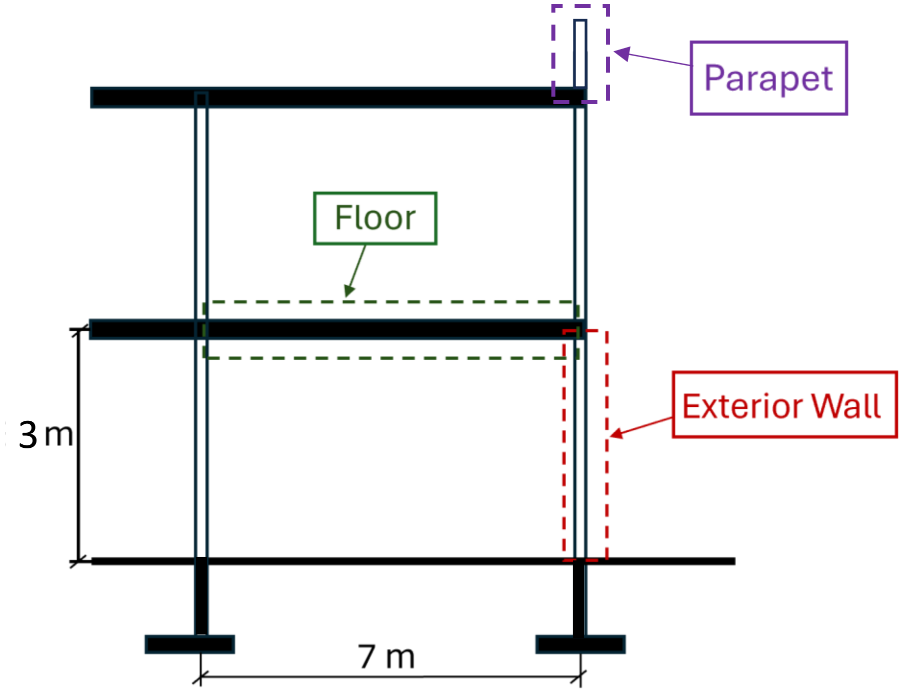

Figure 6: Simplified schematic of wall and roof configuration for the design example of kitchen project.

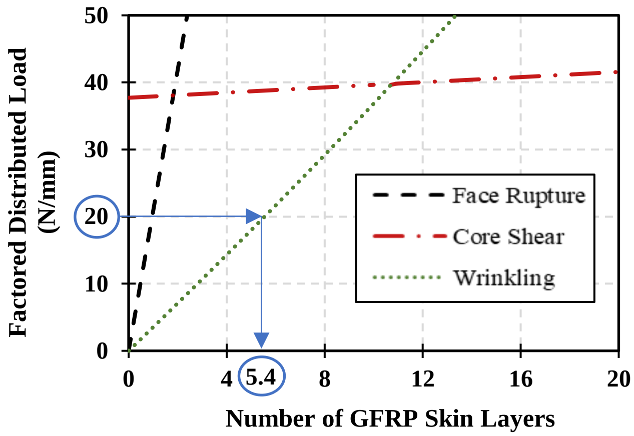

Figure 7: Factored distributed load in bending vs. number of GFRP facing layers for SIPs, highlighting responses to wrinkling, core shear, and face rupture.

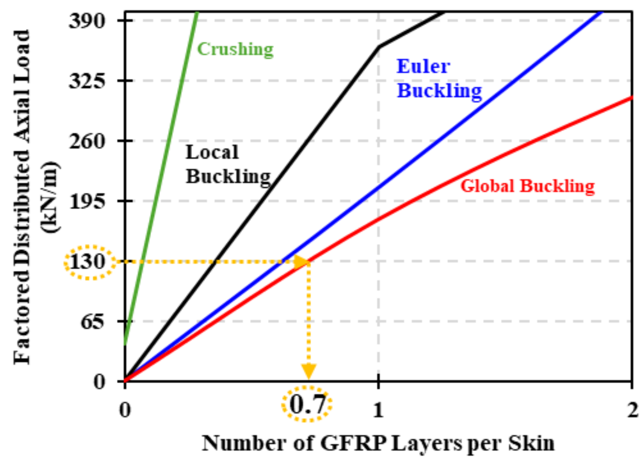

Figure 8: Factored distributed load in axial compression vs. number of GFRP facing layers for SIPs, comparing global buckling predictions using the traditional Euler method (derived from Equation 5) and Allen's modified approach (derived from Equation 7), alongside local buckling (derived from Equation 9) and axial crushing failure modes (derived from Equation 4).